

Effect of oxygen pressure on the orthorhombic-tetragonal transition in the high-temperature superconductor $\text{YBa}_2\text{Cu}_3\text{O}_x$

E. D. Specht, C. J. Sparks, A. G. Dhere, J. Brynestad, O. B. Cavin, and D. M. Kroeger
Oak Ridge National Laboratory, Oak Ridge, Tennessee 37831

H. A. Oye*

F. J. Seiler Research Laboratory, U.S. Air Force Academy, Colorado Springs, Colorado 80840

(Received 8 September 1987; revised manuscript received 28 December 1987)

High-resolution *in situ* x-ray-diffraction measurements were made of the lattice constants of $\text{YBa}_2\text{Cu}_3\text{O}_x$ as it was heated and cooled through the orthorhombic-tetragonal transition at a series of O_2 pressures. The transition is sharp, continuous, and reversible in temperature and pressure. As O_2 pressure is reduced from 1.0 to 0.005 atm, the transition temperature falls from $676 \pm 5^\circ\text{C}$ to $521 \pm 10^\circ\text{C}$ while oxygen content at the transition falls from 6.66 ± 0.01 to 6.59 ± 0.02 . Dilation along the c axis is observed as oxygen is removed. Under helium, an irreversible but time-dependent orthorhombic-to-tetragonal transition occurs during heating.

I. INTRODUCTION

Following the discovery of superconductivity above 90 K in the oxygen-deficient perovskite $\text{YBa}_2\text{Cu}_3\text{O}_x$ (Refs. 1 and 2), several reports have been made of a structural phase transition in the compound.³⁻⁸ Since high-temperature superconductivity is commonly associated with structural instabilities,⁹ it is likely that understanding the structural dynamics of these new superconductors will elucidate understanding of their extraordinarily high superconducting temperatures.

X-ray^{3,4} and neutron⁵ powder diffraction measurements have established an orthorhombic room-temperature structure which transforms upon heating under an oxygen atmosphere to a tetragonal structure with reported orthorhombic-tetragonal transition temperatures ranging from 610°C (Ref. 4) to 750°C (Ref. 3). A reduction in O_2 pressure from 1 to 0.02 atm reduces the transition temperature by about 80°C (Refs. 5 and 6). The magnitude at room temperature of the orthorhombic distortion $\Delta \equiv 2(a-b)/(b+a)$, where a , b , and c are the lattice constants, has been variously reported as 0.0036 (Ref. 10) to 0.018 (Ref. 2).

Such variations in structure are attributed^{11,12} to the temperature and oxygen partial pressure under which the sample is prepared and the rate at which the sample is cooled. In an extreme case, the observation¹³ of a tetragonal structure at room temperature was attributed to rapid cooling through the orthorhombic-tetragonal transition. Heating under a helium or reducing atmosphere has been shown^{4,11,12} to induce an irreversible transition to a tetragonal phase stable to room temperature. As the O_2 treatment varies, the superconducting transition temperature T_c changes. In samples quickly cooled after annealing at various temperatures in air, T_c has been shown^{14,15} to vary with O_2 content. According to Beyers *et al.*,¹¹ samples annealed under either helium or 6 atm O_2 become superconducting at 21 and 60 K, respectively; this apparently conflicts with another report¹² that annealing under 40 atm O_2 increased T_c by 1 K.

Oxygen pressure can have a dramatic effect on both the phase stability and T_c because the oxygen content of $\text{YBa}_2\text{Cu}_3\text{O}_x$ is nonstoichiometric and easily varied. Reported values of x at room temperature for the orthorhombic phase range from 6.8 to 7.0 (Refs. 2, 5, 11, 12, and 14-18). The orthorhombic-tetragonal transition has been reported to occur at a constant value of $x = 6.5$ (Ref. 5) or 6.6 (Ref. 6) between 0.02 and 1 atm.

To better understand the effect of O_2 pressure on the orthorhombic-to-tetragonal transition temperature, we have made high-resolution *in situ* x-ray diffraction measurements as the sample transforms at a series of O_2 pressures ranging from 0.005 to 1 atm. We have carefully measured the lattice constants of a $\text{YBa}_2\text{Cu}_3\text{O}_x$ sample as it is heated in ambients from 1 atm O_2 to helium and back to 1 atm O_2 to check for reversibility, stability, and reproducibility. We report thermogravimetric measurements made on similarly prepared samples which establish O_2 stoichiometry x . Magnetic susceptibility measurements of T_c are reported. We describe our x-ray diffraction data in Sec. II, susceptibility data in Sec. III, thermogravimetric data in Sec. IV, and discuss the implication of these results in Sec. V.

II. X-RAY DIFFRACTION

A. Sample preparation

$\text{YBa}_2\text{Cu}_3\text{O}_x$ was prepared from Y_2O_3 (Morton Thiokol, 99.999%) heated to 1100°C and cooled in a desiccator, BaCO_3 (Johnson Matthey, 99.997%) heated to 275°C in air and cooled in a desiccator, and CuO (Johnson Matthey, 99.999%) heated to 600°C and subsequently cooled in dry O_2 . The substances were transferred to a helium drybox with H_2O , CO_2 , and O_2 content less than 2 ppm, in which all weighing, grinding, and filling into dies was conducted.

Weighed amounts of the starting materials were ground together in an Al_2O_3 mortar, cold pressed into a pellet,

and calcined in O₂, first at 900 °C for 4 h, then at 920 °C for 16 h. The pellet was twice reground, repressed, and sintered, first at 940 °C for 14 h, then 950 °C for 16 h and cooled to room temperature in approximately 10 min. The sample was finally ground into a fine powder for x-ray diffraction measurements, and found to superconduct at 92 K.

B. Data collection

Either silver filings passed through a 325 mesh sieve and mixed with the YBa₂Cu₃O_x powder or the pure platinum heater served as a diffraction reference. The sample was then wetted with toluene and spread in a thin layer on a resistively heated platinum ribbon mounted in a Scintag PAD X high-temperature powder diffraction unit with θ, θ geometry and a copper-anode x-ray tube operated at approximately 2 kW.

The 2θ resolution was 0.050° in the 2θ range of 43–45° where most of the data was collected. The high angular resolution provides accurate lattice constants but makes intensity measurement less reliable by limiting the number of grains diffracting; the sample was finely ground to minimize this effect and to make equilibration more rapid than for a sintered sample. A solid-state detector monitored scattered x rays with a single-channel analyzer set to 7% energy resolution about Cu K α .

Other than the approximately 5 min exposure to air while mounting, the sample was always held under an ambient atmosphere of either pure helium, or oxygen, or a mixture of O₂ with N₂, He, or Ar to a total pressure between 0.25 and 1 atm. Temperature was measured with a Pt/(Pt-10% Rh) thermocouple welded to the back of a 5-mil-thick platinum resistance heater. Temperature calibration of the Pt/(Pt-10% Rh) thermocouple was made at room temperature and at the known 573 ± 1 °C quartz α - β transformation temperature.¹⁹ All temperatures were then read directly from the thermocouple with variations of ± 2 °C over a diffraction scan. This thermocouple reading, thermal expansion data²⁰ on Ag and Pt, and their room-temperature lattice constants²¹ were used to correct sample lattice parameter measurements at temperature for diffractometer alignment errors according to the following formula:

$$a_{\text{sample}}^{\text{correct}} = a_{\text{sample}}^{\text{measured}} + [a_{\text{Pt or Ag}}^{\text{RT, known}} (1 + \Delta L/L)_T - a_{\text{Pt or Ag}}^{\text{measured}}], \quad (1)$$

where RT indicates room temperature and $\Delta L/L$ is the temperature-dependent linear thermal expansion. Values of $a^{\text{RT, known}}$ of 4.0880 Å for Ag and 3.9231 Å for Pt were used with Cu K α_1 = 1.5406 Å. The Ag and Pt (200) diffraction lines within 3.5° and 1.2° 2θ , respectively, of the (006), (020), and (200) sample lines were used in Eq. (1). The 2θ dependence of the correction was less than ± 0.0002 Å over a range of ± 6° 2θ as determined with additional measurement of the Ag(200) and Pt(111) lines. Thus, corrected lattice constants determined on the same sample during a run can be compared to ± 0.0002 Å except near the transition because of broadening of the

diffraction lines, but absolute errors may be close to ± 0.002 Å due to uncertainties in the reported lattice constants of Ag and Pt. Careful calibration of the temperature gradient in the x-ray furnace was undertaken to determine the sharpness of the phase transition. Data in 2 °C steps were taken of the sharp α - β transition in quartz at 573 ± 1 °C (Ref. 19), serving to calibrate both the temperature and gradient of the furnace. After the optimization of thermal shielding, quartz sample thickness was reduced to a minimum, giving an α - β transition occurring over a 5 °C full width at half maximum (FWHM) temperature range in 1 atm O₂. We believe this reflects a gradient from the hotter platinum ribbon to the cooler surface and expect a similar temperature gradient in our YBa₂Cu₃O_x sample. We then measured the temperature gradient as a function of total gas pressure and found ΔT to be ≤ 6 °C FWHM at pressures down to 0.2 atm or 9 °C to 0.1 atm and approximately 100 °C in vacuum. We chose to operate at gas pressures above 0.2 atm to keep the temperature gradient of the sample to approximately 5 °C or less.

The sample was, unless otherwise noted, equilibrated at 700 °C for at least 30 min in each atmosphere to assure oxygen equilibrium, cooled in 25 °C steps, held at least 30 min at each temperature while cooling through the orthorhombic-tetragonal transition, then reheated to check reversibility. Reversibility was observed for samples held no more than an hour at temperatures above

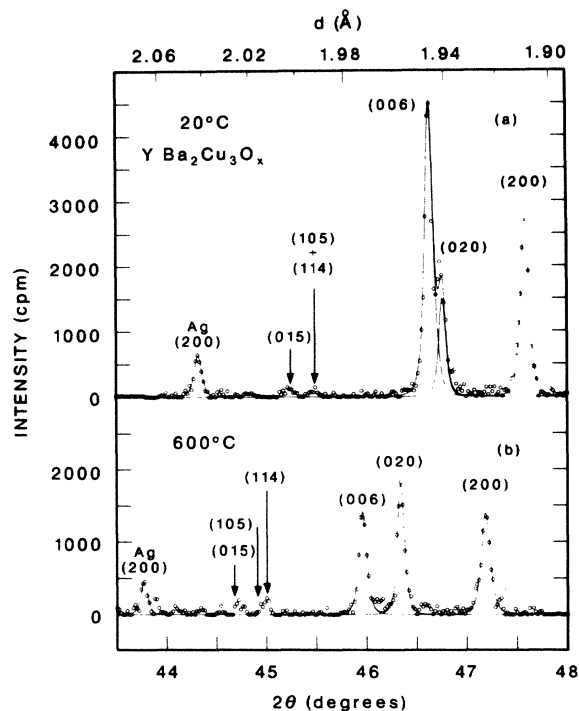


FIG. 1. Diffraction patterns showing 2θ region in which diffraction measurements were made to follow the orthorhombic-to-tetragonal phase transition. All lattice constants were standardized to either the Ag or Pt (200). Solid lines are fits to a Lorentzian-squared line shape. Both are in the orthorhombic phase.

450 °C even under the lowest O₂ pressure. Data collection consisted of a scan through the Ag(200) and (220) peaks or Pt(111) and (200) and the YBa₂Cu₃O_x (006), (020), and (200) peaks. Typical scanning times were approximately 60 to 90 min. To insure that this limited number of peaks gave an accurate measure of the unit-cell dimensions, a scan over 14° < 2θ < 110° was taken at three temperatures for each of three O₂ pressures: The three YBa₂Cu₃O_x peaks chosen were found to give an accurate index to the approximately 50 peaks observed.

C. Results

Typical data are shown in Figs. 1 and 2; Cu Kα₂ has been stripped, leaving diffraction from the 1.5406-Å Kα₁ line, and a linear background of approximately 300 cpm has been subtracted. Solid lines are a least-squares fit to a Lorentzian-squared line shape without correction for instrumental resolution.

Figure 1(a) is the diffraction pattern in the orthorhombic phase as initially prepared by slow furnace cooling in 1 atm O₂. Here the nearly overlapping peaks are the (006) and (020). The splitting between the (020) and the (200) gives an orthorhombic distortion of Δ = 0.017. At 600 °C [Fig. 1(b)], the (006) and (020) have increased their separation due to anisotropic thermal expansion, while Δ is almost unchanged.

Heating through the orthorhombic-tetragonal transition and then cooling, still under 1 atm O₂, we find a single tetragonal phase at 700 °C [Fig. 2(a)], both phases at 675 °C [Fig. 2(b)], and a single orthorhombic phase at 650 °C [Fig. 2(c)] for which diffraction line broadening is apparent in the (020) and (200), but not the (006).

Figure 3 gives the lattice constants of YBa₂Cu₃O_x as a function of temperature at each indicated pressure, corrected as stated above to the Ag and Pt lines. Three

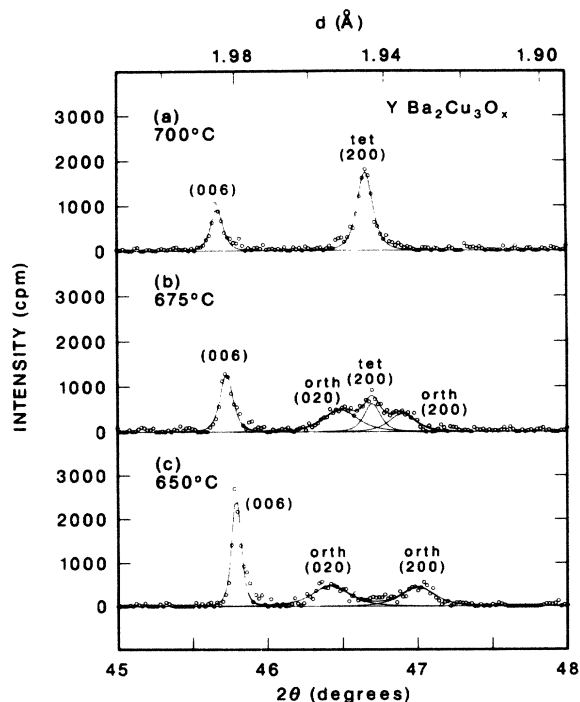


FIG. 2. Diffraction patterns showing YBa₂Cu₃O_x peaks. Solid lines are Lorentzian-squared fits. (a) Tetragonal, (b) coexistence, and (c) orthorhombic phases. Orthorhombic and tetragonal phase (020) and (200) peaks are indicated.

lattice constants are given in the orthorhombic phase, two in the tetragonal; four are shown just at the point where coexistence of both phases exists. The transformation temperature taken from these data are given in Table I. Unit-cell volume expansion calculated from the data of Fig. 3 is plotted in Fig. 4. The trend towards larger cell

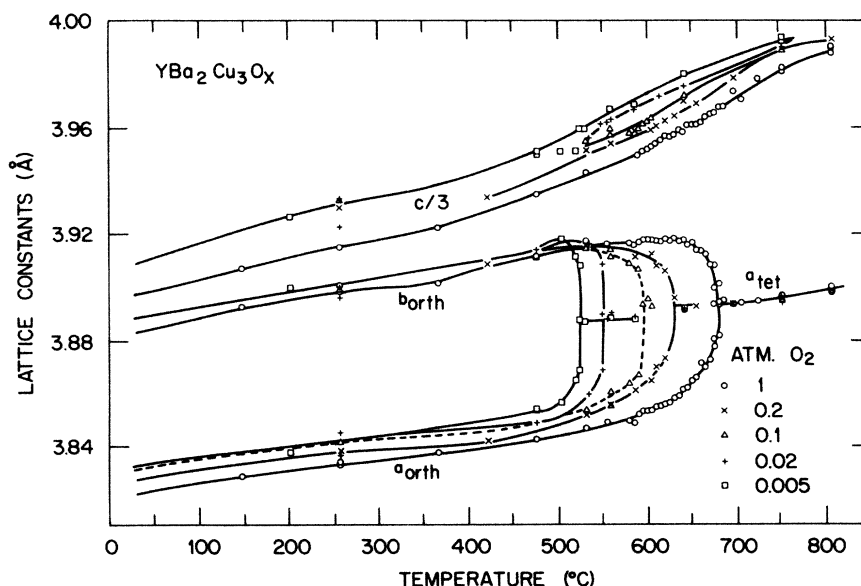


FIG. 3. Lattice constants *a*, *b*, and *c*/3, under various O₂ atmospheres. The orthorhombic-tetragonal transformation decreases with decreasing O₂ pressure. A trend towards larger lattice constants, particularly the *c* direction, is observed as the O₂ pressure is reduced. Lines are guides to the eye.

TABLE I. Orthorhombic-tetragonal phase transformation temperature as a function of O₂ pressure. Numbers in parentheses are twice the standard deviation of the last digit.

O ₂ pressure (atm)	Gas	Transformation temperature (°C)
1	O ₂	676(5)
0.2	air	616(9)
0.1	air	593(8)
0.02	2% O ₂ in He	549(12)
0.005	2% O ₂ in He	521(10)

volume with decreasing O₂ pressure is obvious, but at 800°C the volume becomes independent of O₂ pressure.

Under a helium atmosphere we do not see a reversible transition. The orthorhombic phase produced by cooling to 25°C under O₂ persists up to a temperature of either 460 or 500°C depending on holding time at temperature as the sample is heated (Fig. 5); once the sample is transformed to the tetragonal phase, no further change occurs as it is cooled and reheated in helium. A sample treated at 500°C in an atmosphere of helium and slowly cooled to retain the tetragonal phase at room temperature was then rapidly heated to 385°C under 1 atm O₂ where the transformation to the orthorhombic phase took place over a time period of about 2 h (Fig. 6).

From 0.005 to 1.0 atm O₂, the lattice constants vary reversibly through the orthorhombic-tetragonal transition. As illustrated in Fig. 3, there is a trend towards larger lattice constants as the O₂ pressure is lowered. In particular, we observe a dilation of the *c* axis at lower oxygen pressures and following temperature cycling. The *c* axis of the freshly prepared sample is smaller by $\Delta c/c = 2.9 \times 10^{-3}$ than for all subsequent measurements. There is a similar but smaller trend for the *a* axis and even less so for the *b* axis. This trend is evident in the volume data of Fig. 4, and we attribute this dilation to a small loss in oxygen

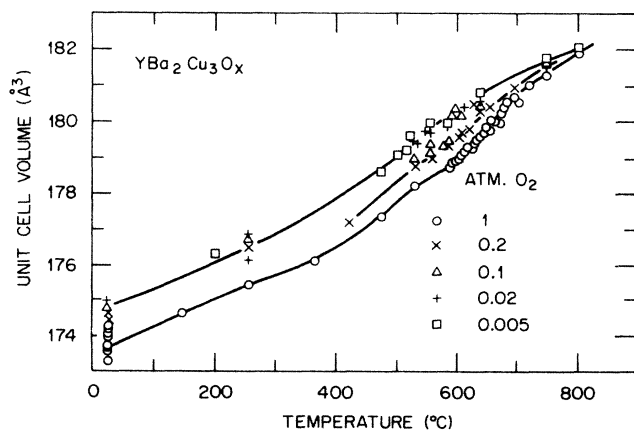


FIG. 4. Unit-cell volume as a function of temperature for various O₂ pressures. Lines are guides to the eye illustrating that an increase in O₂ pressure has little effect on cell volume at 800°C.

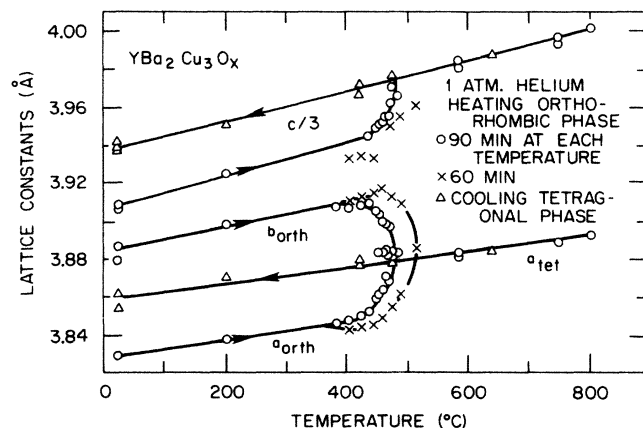


FIG. 5. Lattice constants beginning with the heating of the orthorhombic phase under helium show an irreversible and time-dependent orthorhombic-tetragonal transition with a large *c*-axis spacing change. Lines are guides to the eye.

content of the sample. We observe that temperature- and pressure-cycled samples do not always return to the same values of the lattice constants. Thus, data taken under identical conditions but after cycling the sample do not superimpose well; this lack of reproducibility accounts for most of the scatter in our data.

We examined the time dependence of the diffraction pattern at different temperatures by comparing a scan taken approximately 60 min after a temperature change with one several hours later. In the tetragonal phase we observe a small shift in lattice constants ($\Delta a/a = 8 \times 10^{-4}$, $\Delta c/c = -1.4 \times 10^{-3}$) over a 3-h period under helium at 425°C. We observe a small shift after 2 h at a somewhat higher temperature of 521°C in the orthorhombic-tetragonal coexistence region under 0.005 atm O₂, with $\Delta b/b = -1.3 \times 10^{-3}$. No change in the coexistence line shape [Fig. 2(b)] was observed for a sample held at

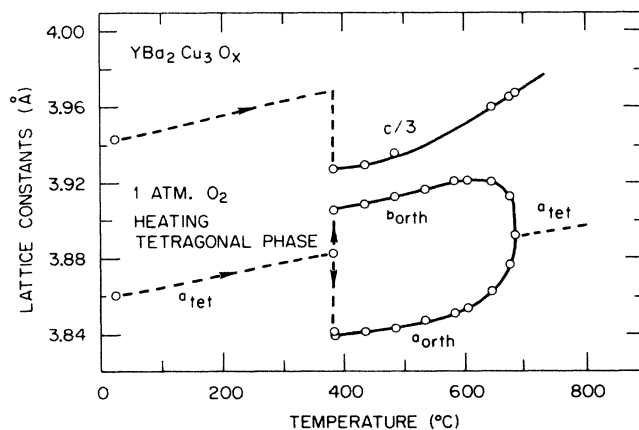


FIG. 6. Lattice constants for the tetragonal phase heated in 1 atm O₂ to 385°C, where it undergoes a kinetic-dependent transformation to the orthorhombic phase in about 2 h then reverts back to the tetragonal phase at 676°C. The dashed line traces the lattice constants of the tetragonal phase taken from Fig. 5.

676 °C under 1 atm O₂ for 5 h. After exposure of the platinum heating element to the sample for several days at temperatures to 800 °C, noticeable roughening and sticking of sample particles to the Pt ribbon had occurred. The powder diffraction pattern had extra peaks (about 2% of the diffracting volume) which were tentatively identified as belonging to the compound Y₂Pt₂O₇.²¹ At temperatures near 700 °C for times less than 6 h no reaction products were identified. Others have also reported a reaction between platinum and YBa₂Cu₃O_x (Ref. 22).

Finally, we consider the peak broadening event in Fig. 2(c). For the freshly prepared orthorhombic sample, all three YBa₂Cu₃O_x peak widths were 0.09° FWHM in 2θ; subtracting in quadrature the 0.05° Δ2θ instrumental resolution gives a width Δq = 2πΔ(2θ)cosθ/λ = 4.9 × 10⁻³ Å⁻¹ at q = 3.2 Å⁻¹. After one cycle through the orthorhombic-tetragonal transition, the width of the (006) does not change, while the (020) and (200) have broadened to 0.25° [Δq = 1.7 × 10⁻² Å⁻¹, Fig. 2(c)]. The sample was cooled from 750 °C increments with approximately 90 min equilibration at each step.

Peak broadening on further cooling depends on cooling rate. If the sample is cooled abruptly to room temperature (~1 sec), the (020) and (200) remain at 0.25° FWHM; when cooled slowly (~1 h), they narrow to approximately 0.14° (Δq = 8.7 × 10⁻³ Å⁻¹). In either case, reheating to 650 °C (just below the transition) reproduces the 0.25° FWHM linewidth.

Due to the large change in the *a* and *b* lattice constants with temperature just below the orthorhombic-tetragonal transition, a 5 °C thermal gradient can produce as much as 0.12° peak broadening. Since this effect is negligible at lower temperatures, the broadening in the (200) and (020) directions is a retention by rapid cooling of the particle size and strain effects induced at temperatures just below the transition. The decreasing width observed on slow cooling is an annealing out of these effects.

III. SUSCEPTIBILITY

Superconducting transition temperatures were determined from the diamagnetic response of the sample in an alternating magnetic field. Specimen material in the form of either 4-mm-diam sintered rods or powder contained in a brass can of similar dimension was placed in an ac field (200 Hz, 1.5 Oe) parallel to the rod axis. With the sample in the normal state, the voltage induced in a pickup coil around the sample was balanced against the signal from a similar but empty coil in the same ac field. This difference was then measured as a function of temperature through the transition. The signal change associated with the transition is proportional to the amount of flux excluded from the sample. For sintered rods, flux exclusion was essentially complete. For powders, the signal at 77 K was about one-half that for the sintered rods. The onset of the inductive transition was taken to be *T_c*.

Figure 7 shows the susceptibility of two samples prepared as for x-ray diffraction, but with the final grinding omitted. One sample was equilibrated in a 1 atm O₂ ambient for 24 h at 950 °C, 8 h at 700 °C, and 16 h at

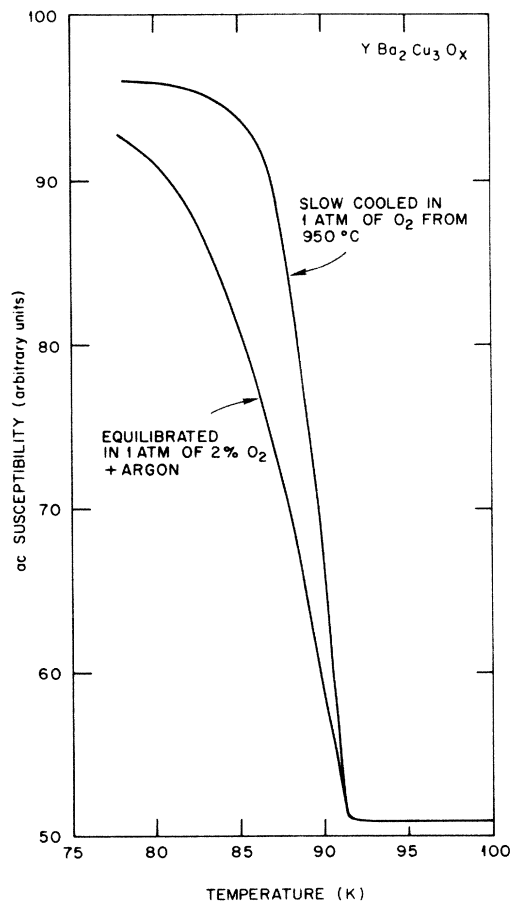


FIG. 7. Magnetic susceptibility of samples prepared in 1.0 and 0.02 atm O₂ showing *T_c* near 91 K.

550 °C; the other in a 0.98 atm Ar-0.02 atm O₂ mixture for 1 h at 725 °C and 3 h at 450 °C. There is no significant difference between their susceptibilities; both show a sharp superconducting transition at 91 K. Samples finely ground as for our x-ray measurements exhibit similar behavior.

IV. THERMOGRAVIMETRY

The weight change of similarly prepared samples was measured as a function of oxygen pressure and temperature with a modified Perkin-Elmer TGA7 thermogravimetric analyzer. The gas flow-through system was disconnected and the furnace chamber was connected to a Mensor quartz manometer and controller which was coupled to a tank with purified oxygen and a mechanical vacuum pump. This allowed attainment of constant pressure in the range 0.007 to 0.74 atm (Colorado Springs' ambient atmospheric pressure). The high-temperature furnace of the TGA7 was utilized with the sample contained in a platinum crucible. The temperature was registered by a Pt-(Pt 10% Rh) thermocouple kept within 2 mm of the sample. The thermocouple was checked against a calibrated Chromel-Alumel thermocouple also placed in the

furnace and the thermocouples agreed within 1°C. A weight calibration was performed according to the manufacturer's specifications. The balance accuracy is given as better than 0.1%, but the weighing precision is 10⁻³%. The pressure controller was calibrated and the absolute accuracy given as 8 × 10⁻⁵ atm at the highest pressure and 7 × 10⁻⁵ atm at the lowest pressures.

Sintered YBa₂Cu₃O_x was prepared as described previously, omitting the final grinding. The furnace with sample was evacuated to 0.007 atm and filled with purified oxygen to 0.74 atm a total of four times to assure that all nitrogen was removed. The temperature after each change was held constant between 40 and 120 min, most often 60 min. An equilibration time of 40 min was found sufficient to ensure the attainment of equilibrium. An absolute scale for the oxygen-atom fraction in the sample was obtained by reducing the sample in 1 atm H₂ at 650°C, assuming the reaction products are Y₂O₃, BaO, and Cu and by measuring the total oxygen weight loss for a known weight of sample.

Shown in Fig. 8 are constant pressure runs performed on a series of samples produced under similar conditions: they agree to within Δx = 0.01. Under 0.737 atm O₂, oxygen content decreases steadily from x = 6.97 at 25°C to x = 6.33 at 935°C, with a break in slope at 661°C, close to the value of 664°C obtained for the orthorhombic-tetragonal transition by interpolating the x-ray diffraction results presented in Fig. 3. As seen in Fig. 3, this transi-

tion temperature drops as O₂ pressure is decreased. For samples equilibrated in 1 atm of O₂ and slowly cooled, values of x are reported to be 6.91 (Ref. 5) from neutron diffraction data; 6.93 ± 0.02 (Ref. 14) from thermogravimetric analysis (TGA) with iodometric titration assuming Ba²⁺, Y³⁺, and O²⁻ to obtain an absolute value; and 6.72 (Ref. 11) from TGA with reduction in 4% H₂ in Ar and assuming the reduction products are Y₂O₃, BaO, and Cu metal. We obtained a value of 6.97 ± 0.01 with a calibration technique of reduction in pure hydrogen and assuming the same reaction products.

Figure 9 shows similar data taken at constant temperature. These data cover the temperature and pressure range over which x-ray diffraction data were obtained. Measurements were made by equilibrating the sample at the highest oxygen pressure (plotted as an open square) then reducing the pressure to the lowest value followed by stepwise increases and holding 5 min at each pressure (plotted as open circles). The sample was then returned to the lowest gas pressure and measured (plotted as an open square) to check reproducibility. With these data we can draw constant oxygen content contours as a function of temperature and O₂ pressure and superimpose them on our x-ray diffraction observations of the orthorhombic and tetragonal phases. This phase diagram is shown in Fig. 10. The estimated error in O₂ concentration, temperature, and pressure of the phase transition is no larger than the data points.

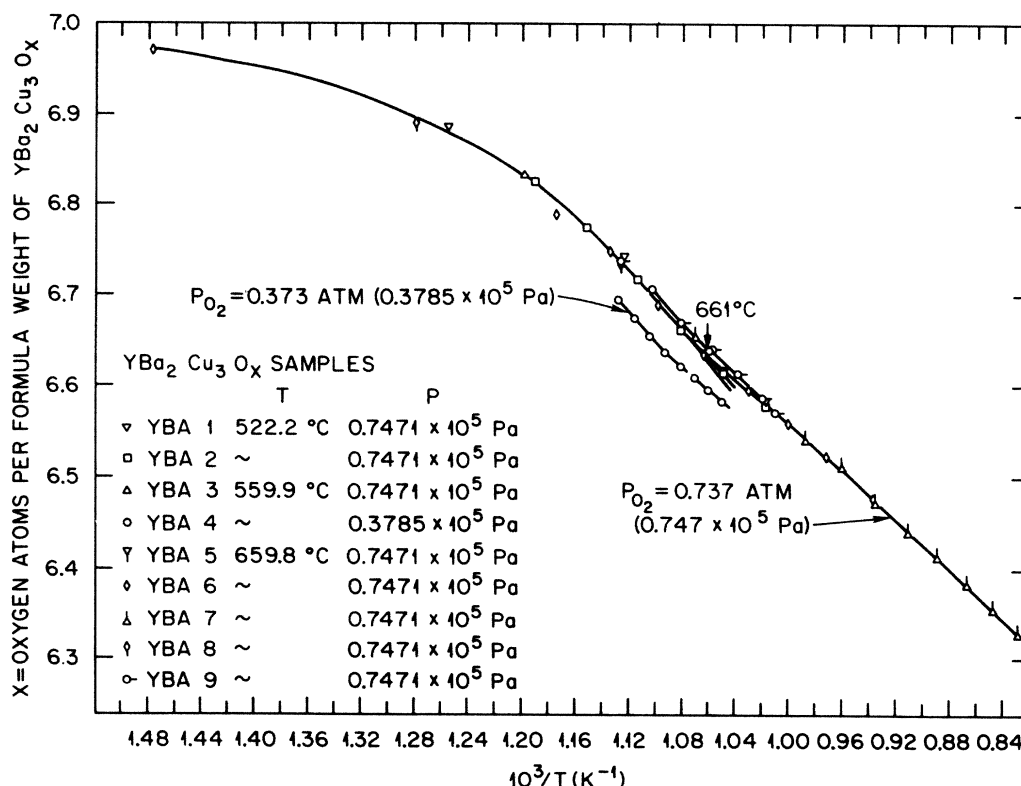


FIG. 8. Thermogravimetric analysis of oxygen content at constant pressure (p) shows correspondence for samples from several batches. Data from constant temperature (t) measurements were superimposed when possible. Lines are guides to the eye.

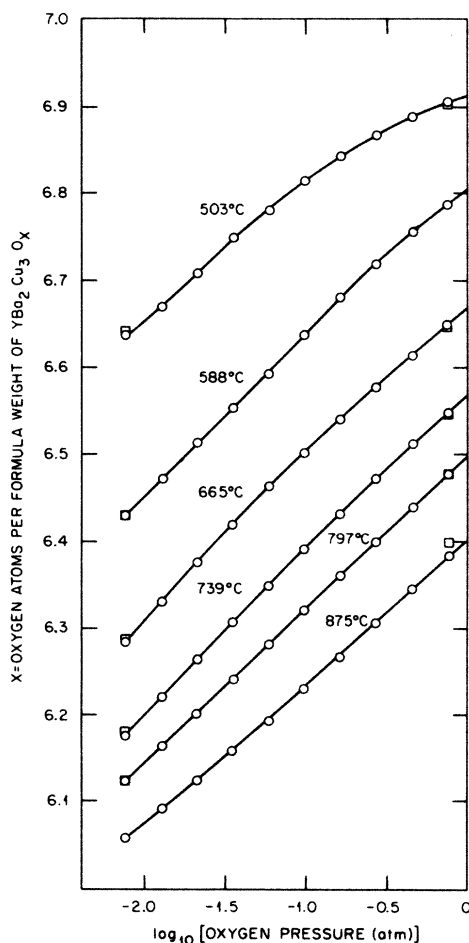


FIG. 9. Oxygen content from TGA analysis at various temperatures and pressures. Open circles are for increasing O_2 pressure while open squares show reproducibility with measurements made initially at the highest pressure and on completion at the lowest pressure.

V. DISCUSSION

A. Lattice constants

As may be seen from the data given in Figs. 3 and 4, the orthorhombic-tetragonal transition temperature decreases as O_2 pressure decreases, and the structure dilates, in particular along the c axis. Oxygen pressure affects the lattice constant a more so than b . The removal of oxygen by equilibrating in helium does reduce a in the tetragonal phase. However, the expansion of c as the oxygen is removed (Fig. 5) is large. In general, c is the lattice parameter most sensitive to oxygen content.

The dependence of the orthorhombic lattice parameters and our thermogravimetric data on O_2 pressure is not consistent with thermogravimetric measurements¹⁴ showing O_2 content $x = 6.93$ at 350°C , constant between 0.01 and 1 atm O_2 . However, some of the difference that we observe in cell volume following either furnace cooling or more rapid *in situ* cooling is attributed to slow O_2 absorption near 400°C , corresponding to the slow kinetics ob-

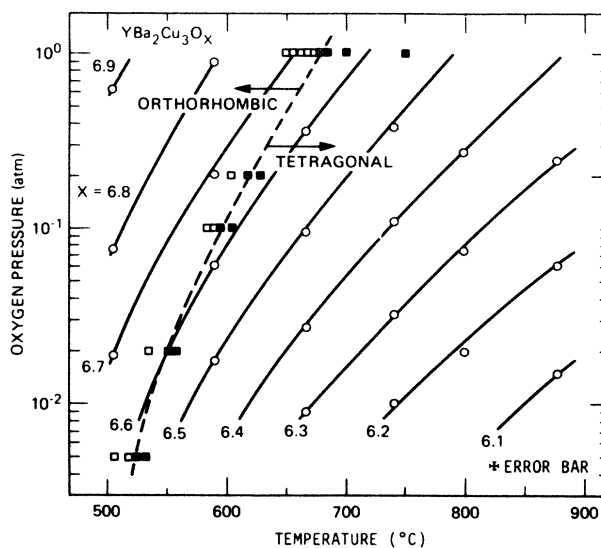


FIG. 10. Structural phase diagram. Open squares indicate orthorhombic diffraction pattern, filled squares indicate tetragonal, and \times -filled squares indicate the point of transformation. Constant oxygen content contours are taken from Fig. 8.

served in our diffraction pattern. More rapidly cooled samples will have even lower oxygen content x and a larger cell volume.

Magnetic susceptibility (Fig. 7) indicates the same superconducting transition temperature for samples annealed in 1.0 and 0.02 atm O_2 , suggesting a room-temperature structure not strongly dependent on oxygen pressure. Similarly, other experiments show that equilibrating in 40 atm of oxygen increased T_c by only 1 K (Ref. 12).

While cooling rate will affect c , neither that nor O_2 pressure greatly changes a or b , so the reported variation in orthorhombic distortion at room temperature must have another explanation. Confirming this, we note that the samples exhibiting the extreme values of $\Delta = 0.0036$ and 0.018 were reportedly prepared under similar conditions.¹⁰ Our value of $\Delta = 0.017$ is in close agreement with those reported most recently.

Table II is a compilation of the crystallographic data obtained from this experiment. The volume of the unit cell derived from the 1 atm O_2 data presented in Fig. 4 shows no obvious inflection points near the transition temperature. Coefficients of thermal expansion, α , for various temperature ranges are listed. Since oxygen loss above 400°C accounts for part of the c -axis expansion, data below that temperature were used so that α reflects thermal expansion at near-constant oxygen content. Thermal expansion data taken in helium for the tetragonal phase reflect constant oxygen content over the entire temperature range. The thermal expansion of the c axis is almost twice that of the a or b axes. We note that the values of α are similar for both the orthorhombic and tetragonal phases.

We observe from Figs. 3 and 5 that the linearly extrapolated a -axis spacing of the tetragonal phase is 0.008 \AA

TABLE II. Unit-cell volume of $\text{YBa}_2\text{Cu}_3\text{O}_x$ in 1 atm of oxygen for various temperatures and values of x . Interpolated values of $c/3$ for 1 atm of oxygen and helium are given. The oxygen content of the oxygen-equilibrated sample varies with temperature where for helium it is fixed at $x = 6.1$. Coefficients of thermal expansion, α , for the orthorhombic and tetragonal phases are given for the sample equilibrated in 1 atm of oxygen and 1 atm of helium, respectively. In the last column the coefficients of c -axis expansion per oxygen atom per formula weight, $\Delta c/c\Delta x$, are listed. The numbers in parentheses are twice the standard deviation of the last digit.

Temperature (°C)	Unit-cell volume ortho. (Å ³)	1 atm oxygen			1 atm helium			Δx oxygen atoms	$\Delta c/c\Delta x$
		x oxygen atoms	$c/3$ ortho. (Å)	α 25–400 °C ortho. (10 ⁻⁶ K ⁻¹)	$c/3$ tet. (Å)	α 25–750 °C tet. (10 ⁻⁶ K ⁻¹)			
20	173.5(2)	6.97(2)	3.893(2)	$\alpha_c = 19(1)$	3.939(2)	$\alpha_c = 21(1)$	0.87(9)	-0.012(2)	
150	174.6(2)	6.97(2)	3.906(2)	$\alpha_a = 11(1)$	3.949(2)	$\alpha_a = 10(1)$	0.87(9)	-0.012(2)	
250	175.5(2)	6.97(2)	3.914(2)	$\alpha_b = 13(1)$	3.957(2)		0.87(9)	-0.012(2)	
350	176.0(2)	6.96(3)	3.921(2)		3.966(2)		0.86(9)	-0.013(2)	
450	177.2(2)	6.95(2)	3.934(2)		3.978(2)		0.85(9)	-0.013(2)	
550	178.4(2)	6.84(2)	3.949(2)		3.984(2)		0.74(9)	-0.012(3)	
650	180.1(2)	6.71(2)	3.962(2)		3.992(2)		0.57(9)	-0.011(3)	
750	181.4(2)	6.56(2)	3.978(2)		4.000(2)		0.48(10)	-0.007(3)	

greater than \sqrt{ab} of the orthorhombic phase. We can understand this asymmetry from the crystallography of the phase transformation obtained from neutron diffraction data.⁵ The copper-oxygen containing plane midway between the two barium atoms has the oxygen atom only along the b axis in the orthorhombic phase. On transforming from the orthorhombic phase where $x \approx 6.65$ in 1 atm O_2 , one-half the O_2 atoms (or $\Delta x = 0.32$) move from the b row to fill 0.32 of the vacant oxygen sites along the a axis. Since the removal of oxygen atoms from the 65% occupied b row produces a smaller contraction ($-\Delta b$) than the expansion (Δa) caused by adding these atoms to a vacant row, the interatomic forces differ depending on the degree of occupation.

A measure of the effect of increasing oxygen content on the contraction of the c axis is given by the parameter $\Delta c/c\Delta x$. A minimum value of $x = 6.1$ for the oxygen content of the helium-treated sample independent of temperature was chosen for the following reasons. Our minimum value of x is near 6.05 and was obtained in $10^{-2.1}$ atm of oxygen at 875 °C. A value of $x = 6.1$ was reported from TGA analysis¹⁴ in 10^{-4} atm of oxygen at a temperature above 650 °C and a value near 6.1 was obtained from neutron diffraction data⁵ in 0.02 atm of oxygen at a temperature near 900 °C. Values of $\Delta c/c\Delta x$ per oxygen ion were found to change from -0.012 at room temperature to -0.007 at 750 °C and are given in Table II.

B. Orthorhombic-tetragonal transition

A measure of the homogeneity of our sample is the abruptness of the observed structural transition. We observed coexistence of the orthorhombic and tetragonal phases over a range of approximately 1 °C after correcting for the temperature gradient. When quartz is substituted for $\text{YBa}_2\text{Cu}_3\text{O}_x$ in our x-ray furnace, we observe coexisting α and β phases over a similar range at 573 °C. Since this transition is known to be sharp, ≤ 1 °C (Ref. 19), we

conclude that the transition observed in $\text{YBa}_2\text{Cu}_3\text{O}_x$ is similarly sharp, ≤ 1 °C, and that a thermal gradient of about 5 °C must exist in the sample.

Our data are consistent with a second-order phase transition. The coefficient of thermal expansion will diverge along the a and b axes as the transition is approached from below. We see broadened orthorhombic phase peaks as we would expect in the presence of a thermal gradient. We observe no peaks with orthorhombic distortion $0 < \Delta < 0.005$; either this is a small first order jump or the broadened peaks become too weak to observe.

While we observe a drop in transition temperature from 676 °C in 1 atm O_2 to 521 °C under a partial pressure of 0.005 atm O_2 (Table I), there is only a slight reduction in the O_2 content at the transition (Fig. 10) from $x = 6.66$ at 1 atm to $x = 6.58$ at 0.005 atm. This result differs from that of Jorgensen *et al.*,⁵ who observe the transition at a constant oxygen content of $x = 6.5$. We report thermogravimetric measurements of total oxygen content, while Jorgensen *et al.* deduce oxygen content from their diffraction pattern; while ours is a more direct measure, it will include any oxygen in grain boundaries or other defects.

Under a partial pressure of oxygen, the transition is reversible so it reflects equilibrium behavior. Under a helium atmosphere, oxygen can only evolve, so we see an irreversible transition reflecting the kinetics of oxygen transport. Our equilibrium measurements show an orthorhombic phase above $x \approx 6.6$, tetragonal below; this is likely to be true even for samples out of equilibrium.

For samples cooled in O_2 then reheated in He, the increase in transition temperature with heating rate (Fig. 5) shows that oxygen evolution occurs in approximately 1 h in the 456–506 °C temperature range. Cooling in He and heating in O_2 shows that oxygen uptake is faster, as the sample transforms to orthorhombic at 400 °C (Fig. 6). Some of this difference may reflect the need for evolved O_2 to diffuse out through helium.

ACKNOWLEDGMENTS

We thank J. D. Jorgensen, W. H. Butler, K. Hisatsune, and J. D. Budai for helpful discussions. H. Yakel was most helpful in the analysis of our data and for comments on the manuscript. The x-ray data in this report were ob-

tained using the x-ray facilities of the High Temperature Materials Laboratory at Oak Ridge National Laboratory. The Research was sponsored by the Division of Materials Sciences, U.S. Department of Energy, under Contract No. DE-AC05-84OR21400 with the Martin Marietta Energy Systems, Inc.

*Permanent address: Norwegian Institute of Technology, Institute of Inorganic Chemistry, 7034 Trondheim, Norway.

- ¹M. K. Wu, J. R. Ashburn, C. J. Torng, P. H. Hor, R. L. Meng, L. Gao, Z. J. Huang, Y. U. Wang, and C. W. Chu, *Phys. Rev. Lett.* **58**, 908 (1987).
- ²R. J. Cava, B. Batlogg, R. B. van Dover, D. W. Murphy, S. Sunshine, T. Siegrist, J. P. Remeika, E. A. Rietman, S. Zahurak, and A. P. Espinosa, *Phys. Rev. Lett.* **58**, 1676 (1987).
- ³I. K. Schuller, D. G. Hinks, M. A. Beno, D. W. Capone II, L. Soderholm, J.-P. Locquet, Y. Bruynseraede, C. U. Segre, and K. Zhang, *Solid State Commun.* **63**, 385 (1987).
- ⁴M. O. Eatough, D. S. Ginley, B. Morosin, and E. L. Venturini, *Appl. Phys. Lett.* **51**, 367 (1987).
- ⁵J. D. Jorgensen, M. A. Beno, D. G. Hinks, L. Soderholm, K. J. Volin, R. L. Hitterman, J. D. Grace, I. K. Schuller, C. U. Segre, K. Zhang, and M. S. Kleefisch, *Phys. Rev. B* **36**, 3608 (1987).
- ⁶H. M. O'Bryan and P. K. Gallagher, *Adv. Ceram. Mater.* **2**, 640 (1987).
- ⁷E. Takayama-Muromachi, Y. Uchida, K. Yukino, T. Tanaka, and K. Kato, *Jpn. J. Appl. Phys.* **26**, L665 (1987).
- ⁸K. Yukino, T. Sato, S. Ooba, M. Ohra, F. P. Okamura, and A. Ono, *Jpn. J. Appl. Phys.* **26**, L869 (1987).
- ⁹B. T. Matthias, in *Superconductivity in d- and f-Band Metals*, edited by D. H. Douglas (AIP, New York, 1972), p. 367.
- ¹⁰T. Siegrist, S. Sunshine, D. W. Murphy, R. J. Cava, and S. M. Zahurak, *Phys. Rev. B* **35**, 7137 (1987).
- ¹¹R. Beyers, G. Lim, E. M. Englar, V. Y. Lee, M. L. Ramirez, R. J. Savoy, R. D. Jacowitz, T. M. Shaw, S. La Placa, R. Boehme, C. C. Tsuei, Sung I. Park, M. W. Shafer, and W. J. Gallagher, *Appl. Phys. Lett.* **51**, 614 (1987).
- ¹²J. M. Tarascon, W. R. McKinnon, L. H. Greene, G. W. Hull, and E. M. Vogel, *Phys. Rev. B* **36**, 226 (1987).
- ¹³R. M. Hazen, L. W. Finger, C. T. Prewitt, N. L. Ross, H. K. Mao, C. G. Hadjicacos, P. H. Hor, R. L. Meng, and C. W. Chu, *Phys. Rev. B* **35**, 7238 (1987).
- ¹⁴K. Kishio, J. Shimoyama, T. Hasegawa, K. Kitazawa, and K. Fueki, *Jpn. J. Appl. Phys.* **26**, L1228 (1987).
- ¹⁵E. Takayama-Muromachi, Y. Uchida, M. Ishii, T. Tanaka, and K. Kato, *Jpn. J. Appl. Phys.* **26**, L1156 (1987).
- ¹⁶P. K. Gallagher, *Adv. Ceram. Mater.* **2**, 632 (1987).
- ¹⁷J. J. Capponi, C. Chaillout, A. W. Hewat, P. Lejay, M. Marezio, N. Nguyen, B. Raveau, J. L. Soubeyrcux, J. L. Tholence, and R. Tournier, *Europhys. Lett.* **3**, 1301 (1987).
- ¹⁸M. A. Beno, L. Soderholm, D. W. Capone II, D. G. Hinks, J. D. Jorgensen, I. K. Schuller, C. U. Segre, K. Zhang, and J. D. Grace, *Appl. Phys. Lett.* **51**, 57 (1987).
- ¹⁹R. J. Ackermann and C. A. Sorrell, *J. Appl. Crystallogr.* **7**, 461 (1974).
- ²⁰*Thermophysical Properties of Matter*, edited by Y. S. Touloukian (IFI/Plenum, New York, 1975), Vol. 12.
- ²¹H. R. Hoekstra and F. Gallagher, *Inorg. Chem.* **7**, 2553 (1968).
- ²²J. S. Swinnea and H. Steinfink, *J. Mater. Res.* **2**, 424 (1987).